
Differentially private training of residual networks with scale normalisation

Helena Klause¹ Alexander Ziller^{1,2} Daniel Rueckert^{1,3} Kerstin Hammernik^{1,3} Georgios Kaissis^{1,2,3}

Abstract

The training of neural networks with Differentially Private Stochastic Gradient Descent offers formal Differential Privacy guarantees but introduces accuracy trade-offs. In this work, we propose to alleviate these trade-offs in residual networks with Group Normalisation through a simple architectural modification termed *ScaleNorm* by which an additional normalisation layer is introduced after the residual block’s addition operation. Our method allows us to further improve on the recently reported state-of-the-art on CIFAR-10, achieving a top-1 accuracy of 82.5% ($\epsilon = 8.0$) when trained *from scratch*.

1. Introduction

Differentially Private Stochastic Gradient Descent (DP-SGD) (Abadi et al., 2016) is arguably the most widely utilised technique for training deep neural networks with Differential Privacy (DP) guarantees. Although it offers formal guarantees of privacy to the individuals whose data is used to train the model, its utilisation results in accuracy trade-offs. These trade-offs are undesirable, especially in critical domains such as medicine where both high diagnostic accuracy and strong privacy guarantees are required, prompting the development of methods to alleviate these privacy-utility trade-offs. In the current work, we focus on computer vision tasks, which represent one of the broadest application areas for deep learning.

Residual networks (ResNets) (He et al., 2016) are a standard architecture in computer vision. The residual block, their core architectural building block, has since become a standard component of architectures responsible for several victories in the ImageNet (ILSVR) challenge (Deng et al., 2009). Moreover, despite newer works introducing novel

architectures which outperform the original ResNets, it has recently been shown that their performance can be comparable to current-generation vision models in challenging tasks (Wightman et al., 2021) if trained appropriately. The combination of ResNets and Differentially Private Stochastic Gradient Descent (DP-SGD) thus appears as a promising direction for privately training computer vision models. Indeed, both of the very recently reported successful applications of DP-SGD to the ImageNet dataset were achieved using some variation of the ResNet architecture (Kurakin et al., 2022; De et al., 2022).

In the current work, we observe and address a phenomenon arising in the training of ResNets with DP-SGD, which we term *scale mixing*: Inside a residual block, the activations flowing through the convolutional path are normalised, however the activations flowing through the residual path are not. This leads to impaired convergence and reduced test-set accuracy both in non-DP training and with DP-SGD, but is substantially more pronounced with DP-SGD.

Contributions and overview of the paper Our key contribution is the introduction of an architectural adaptation to the residual block, which we term *scale normalisation* (ScaleNorm). ScaleNorm fixes the scale mixing problem and empirically leads to improved convergence, which we investigate in Section 3.1. Experimentally, we demonstrate the superiority of ResNets with ScaleNorm to regular ResNets on several image benchmark tasks (CIFAR-10, ImageNette, TinyImageNet) in Section 3.2, where we show that—combined with recently introduced training adaptations—we achieve state-of-the-art top-1 accuracy on CIFAR-10 when trained *from scratch*.

2. Prior work

The attempt to alleviate privacy-utility trade-offs in DP-SGD has been the subject of two distinct lines of work. We will focus exclusively on the works investigating the DP-SGD algorithm as presented in Abadi et al. (2016) and omit works relying on modifications to the DP-SGD algorithm or alternative techniques for obtaining improved accuracy (such as Zhu et al. (2020) or Papernot et al. (2018)).

The first approach to improving the training outcome of DP-SGD models is **transfer learning**, that is, *fine-tuning*

¹Chair for AI in Medicine, Technical University of Munich, Germany ²Department of Radiology, Technical University of Munich, Germany ³Department of Computing, Imperial College London, United Kingdom. Correspondence to: Georgios Kaissis <g.kaissis@tum.de>.

a network which has been pre-trained on public data (Luo et al., 2021; Davody et al., 2021; Tramèr & Boneh, 2021). Such works are able to leverage pre-trained representations (or, in the case of Tramèr & Boneh (2021), fixed features from wavelet transforms). This approach has several major benefits: The quality of non-privately learned representations is higher, enabling the practitioner to only train a subset of the network’s layers with DP-SGD, which is both faster and leads to improved accuracy. Moreover, Batch Normalisation (BN) layers can be used in the part of the network that is not trained, as they remain *frozen*.

Our work studies a different situation in which transfer learning is not possible or ineffective, and networks are trained *from scratch*. Such a scenario can arise in cases of a large domain discrepancy between the pre-training dataset and the task at hand (e.g. high-dimensional medical imaging) or because the pre-training dataset is itself sensitive in nature. Moreover, omitting pre-training allows us to empirically observe the training behaviour of the network, which is of independent interest. Two possibilities exist to improve the convergence properties and test-set accuracy. The first are **training adaptations** such as large-batch training (Dörmann et al., 2021), augmentation multiplicity (Fort et al., 2021) or Polyak-Ruppert/exponential weight averaging (Polyak & Juditsky, 1992; Ruppert, 1988; Tan & Le, 2019). These techniques were very recently combined by (De et al., 2022) to achieve the state-of-the art with DP-SGD on ImageNet and CIFAR-10. The second possibility are **architectural adaptations**. These can take the form of adapting the architecture from the ground up, such as Morsbach et al. (2021) and Papernot et al. (2020), who support the hypothesis that specialised architectures for use with DP are required to be designed. A less complicated route is making modifications to *existing* architectures, for example by replacing Batch Normalisation with alternatives such as Group Normalisation (which is mandatory for maintaining DP guarantees) or exchanging the activation functions (Papernot et al., 2021). Our work takes cues from both aforementioned categories, as we modify an existing architecture to improve its performance under DP. In addition, we combine the resulting improved architecture with the training adaptations presented by De et al. (2022) to further improve our results.

3. Methods and Results

3.1. Scale mixing and ScaleNorm

We begin by discussing the origins of the scale mixing problem in ResNets. Figure 1A shows a conventional residual block. The residual path’s activations (V_R) are the immediate output of the previous layer and are scaled (i.e. distributed) differently from the convolutional path’s activations (V_F), which undergo normalisation twice. The

addition operation at the end of the block *mixes* the scales of the two activations, which skews the distributions of the outputs (V_A). Figure 2 (top row) demonstrates this behaviour. ScaleNorm modifies the residual block to include an additional normalisation layer after the addition function (Figure 1B), which re-normalises the outgoing activations V_A . Empirically, this has several beneficial effects. It renders the activations V_A more symmetric about the mean and returns their standard deviation to 1, which has been noted in previous works as a desirable property for training stability (Glorot & Bengio, 2010; Zhang et al., 2019). Moreover, we experimentally found ResNets with ScaleNorm (ScaleResNets) to show substantially improved convergence compared to regular ResNets, as exemplarily shown in Figure 3. This knowledge enables practitioners to *save privacy budget* by training their networks for fewer epochs or with more noise. Beyond improving the activation distributions, we conjecture ScaleNorm to also smoothen the optimisation landscape. Experimentally, the ScaleResNet-9 architecture used in the experiments below has a significantly lower value of the Hessian trace (6637.3) compared to the regular ResNet-9 (9045.7), a slightly lower condition number ($2,1 \cdot 10^{-3}$ vs $2,3 \cdot 10^{-3}$), fewer negative Hessian eigenvalues (115 vs. 119) and lower maximum Hessian eigenvalues (2654.2 vs. 3920.4), indicating a lower curvature of the loss landscape at the convergence point. Of note, ScaleResNets consistently performed better than regular ResNets even without DP-SGD, but the effect was negligible (ca. 0.5% accuracy advantage), which explains why this architectural modification is not standard in non-private deep learning literature. Details of the loss landscape experiments and non-private training can be found in the Appendix.

3.2. Experiments

We assume familiarity with the DP-SGD algorithm (Abadi et al., 2016). Unless otherwise indicated, all experiments below were conducted in triplicate with fixed random seeds selected randomly in advance.

3.2.1. EXPERIMENTS WITH (SCALE)RESNET-9

DP-SGD is resource-intensive and the noise added per step scales proportionally to the number of (trainable) model parameters (Subramani et al., 2021). Thus, we chose to construct a shallow nine-layer ResNet with 2 447 946 parameters for the following experiments. We term this architecture ResNet-9, or ScaleResNet-9 when ScaleNorm was used. The architecture includes Group Normalisation (GN) layers per default. Details of the architectural design and a comparison with ResNet-50, supporting the choice of a smaller model for the following experimental evaluation, can be found in the Appendix. We evaluated the effect of ScaleNorm on CIFAR-10 at an image size of 32×32

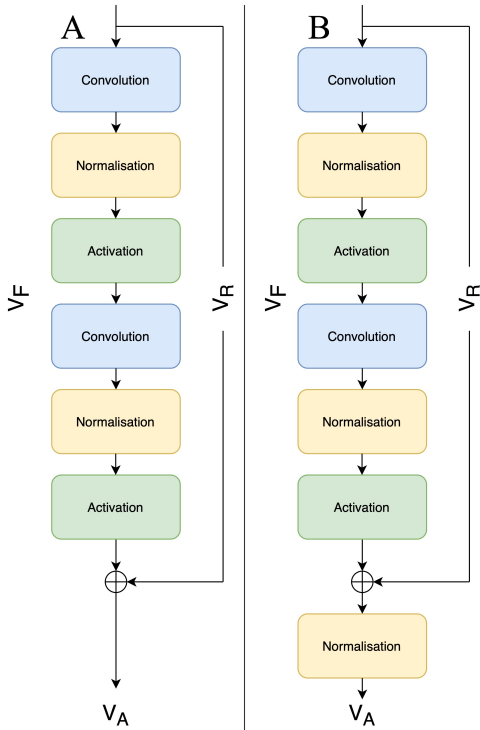


Figure 1. Schematic representation of a residual block (A) vs. a residual block with ScaleNorm (B). Observe the additional normalisation after the addition operation. V_R : Residual path, V_F : Convolutional path, V_A : Activation.

(Krizhevsky et al., 2009), Tiny ImageNet¹ at a size of 64×64 and the 2019 version of ImageNette (Howard, 2019), a subset of 10 ImageNet classes, at an image size of 160×160 . We trained the CIFAR-10 and ImageNette networks for 50 epochs and the Tiny ImageNet network for 90 epochs with an L_2 -norm bound (clipping threshold) of 1.5 using an expected lot (batch) size of 1024 with the NAdam optimiser (Dozat, 2016) at a learning rate of 0.001. We employed a constant learning rate schedule with reduction by half upon stagnation of the validation loss for more than three epochs. We performed a hyperparameter search over the optimal number of GN groups from 1 (equivalent to Layer Normalisation) to the number of channels (equivalent to Instance Normalisation) and intermediate values of 16, 32, 64. Hyperparameter searches were conducted using the *Optuna* package (Akiba et al., 2019) with the *Tree-structured Parzen Estimator* search strategy and the *threshold* pruner. We reset the privacy budget for each hyperparameter search run similar to Kurakin et al. (2022); De et al. (2022), which we note to not preserve DP. ϵ was calculated at a δ of 10^{-5} using the Rényi DP accountant of the *Opacus* package (Yousefpoor et al., 2021). We performed the experiments on CIFAR-10 and ImageNette at three privacy levels: 2.89 (similar to

¹available from <http://cs231n.stanford.edu/>

Tramèr & Boneh (2021)), 7.42 (similar to Dörmann et al. (2021)) and 9.88 (similar to Kurakin et al. (2022)). Tiny ImageNet was trained at $\epsilon \in (5, 10, 70)$ similar to Kurakin et al. (2022) because the dataset is very difficult to train to acceptable accuracy from scratch with DP-SGD with lower ϵ , similar to ImageNet itself, as seen in Kurakin et al. (2022); De et al. (2022). Table 1 summarises our results on CIFAR-10, ImageNette and Tiny ImageNet, respectively.

CIFAR-10			
ϵ	2.89	7.42	9.88
ScaleNorm	65.6	71.8	73.0
No ScaleNorm	65.0	71.4	72.4
ImageNette			
ϵ	2.89	7.42	9.88
ScaleNorm	56.6	64.8	67.1
No ScaleNorm	55.5	63.8	65.0
Tiny ImageNet			
ϵ	5	10	70
ScaleNorm Top-1	15.2	19.4	25.8
No ScaleNorm Top-1	14.2	18.7	24.7
ScaleNorm Top-5	36.0	41.8	50.8
No ScaleNorm Top-5	34.4	40.5	48.3

Table 1. Summary of results on CIFAR-10, ImageNette and Tiny ImageNet. All results are median accuracies (in %) of three runs.

ScaleResNet-9 consistently outperformed the regular ResNet on all tasks. An even stronger separation was observed when comparing the best (instead of the median) models of the three repetitions; these results can be found in the Appendix.

3.2.2. EXPERIMENTS WITH (SCALE)WIDERESNET-16/4

During the preparation of our manuscript, De et al. (2022) published a study utilising a number of training adaptations on top of the WideResNet (WRN) architecture with 16 layers and a width factor of 4 (WRN-16/4, 2752506 parameters) to obtain a top-1 accuracy of 81.4% at an ϵ of 8.0. Examining Table 2 of De et al. (2022), we observe that the greatest accuracy improvement is derived from applying the *augmentation multiplicity* and *weight averaging* training adaptations, whereas the “baseline” accuracy without these adaptations is comparable to our results mentioned above (71.2%). To therefore examine whether larger ResNets also benefit from ScaleNorm and from incorporating the aforementioned training adaptations, we utilised the identical WRN-16/4 architecture, which we also modified to include ScaleNorm after each residual block (ScaleWRN-16/14), and identical training settings. These results were tested on

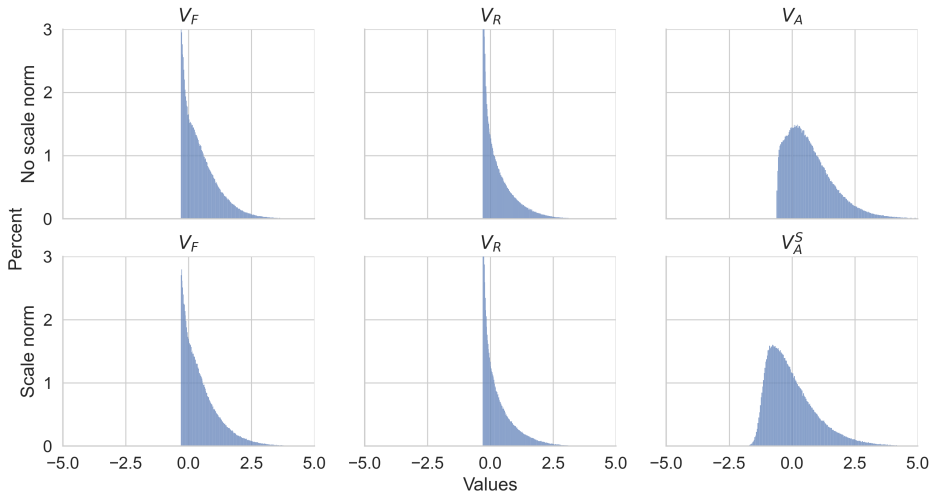


Figure 2. Activation histograms of a ResNet (top row) vs. a ScaleResNet (bottom row) residual block. Observe that the activations output by V_A (top right) are markedly asymmetric with substantial mass on the positive side (sample average: 0.72, standard deviation: 0.76), whereas the activations output by the scale normalisation operation V_A^S (bottom right) are more symmetric about the sample mean of 0 and have unity standard deviation.

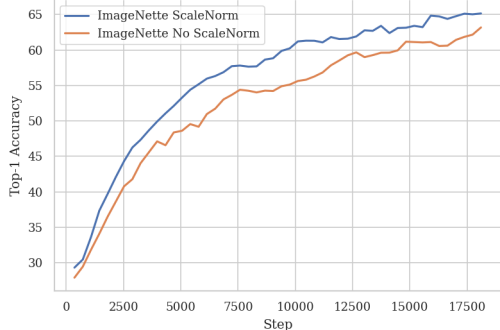


Figure 3. Exemplary training dynamics of a ScaleResNet (blue curve) vs. a regular ResNet (orange curve) in terms of test accuracy on the ImageNet dataset. Observe the markedly improved convergence properties of the ScaleResNet.

the CIFAR-10 test set and are summarised in Table 2.

The ScaleWRN-16/4 architecture achieved an accuracy of 82.5%, outperforming the standard WRN-16/4 (81.25%) and further improving on the results by De et al. (2022) to achieve a (to our knowledge) new state of the art result. We remark that training the ScaleResNet-9 architecture discussed in the previous section requires approximately 20 minutes on a single NVidia Quadro RTX 8000 GPU. Training with the adaptations proposed by De et al. (2022) incurs a massive increase in training time to over 16 hours on a dual-GPU system, which should be weighed against the ca.

	WRN-16/4 ($\epsilon=8.0$)	ResNet-9 ($\epsilon=7.42$)
ScaleNorm	82.5	71.8
No ScaleNorm	81.25	71.4
Training time	963 min	22 min

Table 2. Accuracy (in %) and training time comparison between ResNet-9 and WideResNet-16/4 with and without ScaleNorm. WRN-16/4 was trained with the adaptations proposed by De et al. (2022), which drastically increase training time.

10% accuracy increase from a resource efficiency point of view, and prompts further investigation into software and hardware optimisations for DP-SGD.

4. Discussion and Conclusion

The broad implementation of Differential Privacy (DP) to large-scale computer vision tasks will require tackling the privacy-utility trade-offs inherent to DP-SGD. Our work introduces ScaleNorm, an architectural modification which substantially improves the accuracy of ResNets trained with DP. In future work, we intend to supplement our findings with data on similar architectures such as DenseNets, to clarify the interplay of ScaleNorm with other architectural components such as activation functions or initialisation, and to theoretically investigate its effect on training dynamics.

References

- Abadi, M., Chu, A., Goodfellow, I., McMahan, H. B., Mironov, I., Talwar, K., and Zhang, L. Deep learning with differential privacy. In *Proceedings of the 2016 ACM SIGSAC conference on computer and communications security*, pp. 308–318, 2016.
- Akiba, T., Sano, S., Yanase, T., Ohta, T., and Koyama, M. Optuna: A next-generation hyperparameter optimization framework. In *Proceedings of the 25th ACM SIGKDD International Conference on Knowledge Discovery and Data Mining*, 2019.
- Davody, A., Adelani, D. I., Kleinbauer, T., and Klakow, D. On the effect of normalization layers on differentially private training of deep neural networks. *arXiv preprint 2006.10919*, 2021.
- De, S., Berrada, L., Hayes, J., Smith, S. L., and Balle, B. Unlocking high-accuracy differentially private image classification through scale. *arXiv*, 2022. doi: 10.48550/ARXIV.2204.13650.
- Deng, J., Dong, W., Socher, R., Li, L.-J., Li, K., and Fei-Fei, L. Imagenet: A large-scale hierarchical image database. In *2009 IEEE conference on computer vision and pattern recognition*, pp. 248–255. Ieee, 2009.
- Dörmann, F., Frisk, O., Andersen, L. N., and Pedersen, C. F. Not all noise is accounted equally: How differentially private learning benefits from large sampling rates. In *2021 IEEE 31st International Workshop on Machine Learning for Signal Processing (MLSP)*, pp. 1–6, 2021.
- Dozat, T. Incorporating Nesterov Momentum into Adam. *ICLR Workshop Track*, 2016.
- Fort, S., Brock, A., Pascanu, R., De, S., and Smith, S. L. Drawing multiple augmentation samples per image during training efficiently decreases test error. *arXiv*, 2021. doi: 10.48550/ARXIV.2105.13343.
- Glorot, X. and Bengio, Y. Understanding the difficulty of training deep feedforward neural networks. In *Proceedings of the thirteenth international conference on artificial intelligence and statistics*, pp. 249–256. JMLR Workshop and Conference Proceedings, 2010.
- He, K., Zhang, X., Ren, S., and Sun, J. Deep residual learning for image recognition. In *Proceedings of the IEEE conference on computer vision and pattern recognition*, pp. 770–778, 2016.
- Howard, J. Imagenette, 2019. URL <https://github.com/fastai/imagenette>.
- Krizhevsky, A., Hinton, G., et al. Learning multiple layers of features from tiny images. *Technical Report*, 2009.
- Kurakin, A., Song, S., Chien, S., Geambasu, R., Terzis, A., and Thakurta, A. Toward training at imagenet scale with differential privacy. *arXiv*, 2022.
- Luo, Z., Wu, D. J., Adeli, E., and Fei-Fei, L. Scalable differential privacy with sparse network finetuning. In *2021 IEEE/CVF Conference on Computer Vision and Pattern Recognition (CVPR)*, pp. 5057–5066, 2021.
- Misra, D. Mish: A self regularized non-monotonic activation function. *arXiv*, 2020.
- Morsbach, F., Dehling, T., and Sunyaev, A. Architecture matters: Investigating the influence of differential privacy on neural network design. *CoRR*, abs/2111.14924, 2021.
- Papernot, N., Song, S., Mironov, I., Raghunathan, A., Talwar, K., and Erlingsson, U. Scalable private learning with PATE. *arXiv preprint arXiv:1802.08908*, 2018.
- Papernot, N., Chien, S., Song, S., Thakurta, A., and Erlingsson, U. Making the shoe fit: Architectures, initializations, and tuning for learning with privacy, 2020. URL <https://openreview.net/forum?id=rJg851rYwH>.
- Papernot, N., Thakurta, A., Song, S., Chien, S., and Erlingsson, U. Tempered sigmoid activations for deep learning with differential privacy. *Proceedings of the AAAI Conference on Artificial Intelligence*, 35(10):9312–9321, 2021.
- Polyak, B. T. and Juditsky, A. B. Acceleration of stochastic approximation by averaging. *SIAM journal on control and optimization*, 30(4):838–855, 1992.
- Ruppert, D. Efficient estimations from a slowly convergent robbins-monro process. Technical report, Cornell University Operations Research and Industrial Engineering, 1988.
- Subramani, P., Vadivelu, N., and Kamath, G. Enabling fast differentially private sgd via just-in-time compilation and vectorization. *Advances in Neural Information Processing Systems*, 34, 2021.
- Tan, M. and Le, Q. Efficientnet: Rethinking model scaling for convolutional neural networks. In *International conference on machine learning*, pp. 6105–6114. PMLR, 2019.
- Tramèr, F. and Boneh, D. Differentially private learning needs better features (or much more data). In *9th International Conference on Learning Representations, ICLR 2021*, 2021.
- Wightman, R., Touvron, H., and Jégou, H. Resnet strikes back: An improved training procedure in TIMM. *arXiv*, 2021.

Yao, Z., Gholami, A., Keutzer, K., and Mahoney, M. PyHessian: Neural Networks Through the Lens of the Hessian. *arXiv*, December 2019.

Yousefpour, A., Shilov, I., Sablayrolles, A., Testuggine, D., Prasad, K., Malek, M., Nguyen, J., Ghosh, S., Bharadwaj, A., Zhao, J., Cormode, G., and Mironov, I. Opacus: User-friendly differential privacy library in PyTorch. *arXiv preprint arXiv:2109.12298*, 2021.

Zhang, H., Dauphin, Y. N., and Ma, T. Residual learning without normalization via better initialization. In *International Conference on Learning Representations*, 2019.

Zhu, Y., Yu, X., Chandraker, M., and Wang, Y.-X. Private-KNN: Practical differential privacy for computer vision. In *Proceedings of the IEEE/CVF Conference on Computer Vision and Pattern Recognition*, pp. 11854–11862, 2020.

Appendix

A. Details on training dynamics and Hessian analysis

To analyse the Hessian of the trained network, we used the *PyHessian* package (Yao et al., 2019). For eigenvalue computation, we used the power iteration method with 1000 iterations and a maximum tolerance of 0.001. For computing the Hessian trace, we used Hutchinson’s method with 1000 iterations and a tolerance of 0.001.

B. Non-private ScaleResNet training

To assess whether ScaleNorm also improves convergence and test-set accuracy in the non-private setting, we trained the ResNet-9 architecture with Batch Normalisation (instead of the default Group Normalisation) on the CIFAR-10 dataset. Over three runs, the ScaleResNet-9 achieved a median test-set accuracy of 89.8, whereas the regular ResNet-9 reached a test set accuracy of 89.3. We empirically observed the training of the ScaleResNet to be slightly more stable, which we attributed to the additional mild regularising effect of the additional BN layers. Through this experiment, we empirically conclude that –whereas ScaleNorm minimally benefits non-DP training– further evaluation is required to assess whether a recommendation to use ScaleNorm outside of DP-SGD is warranted.

C. Details on the ResNet-9 architecture

The ResNet-9 architecture consists of nine-layers and includes 2 447 946 parameters. The network consists of two convolutional blocks (64 and 128 filters) followed by one residual block with 128 filters, two convolutional blocks with 256 filters each, a residual block with 256 filters, a global Max Pooling layer and a fully connected layer with 1024 units. We utilised *Mish* activation functions (Misra, 2020) throughout the network. Every convolutional block consists of a convolutional layer followed by an activation and a Group Normalisation layer. For networks with ScaleNorm, the additional normalisation operations follow directly after the residual blocks. An implementation of the architecture using the PyTorch machine learning package can be found at <https://gist.github.com/gkaissis/6db6b7271f93d3459263b6978cfd4146>. We note that the code assumes a CPython version ≥ 3.9 . Users of prior versions must replace the type annotation on line 41 with `typing.Tuple`.

D. Comparison with ResNet-50

We experimentally compared the performance of ResNet-9 to ResNet-50 on the ImageNette dataset to investigate whether the larger architecture would offer benefits due to higher learning capacity. We found that, although ScaleResNet-50 outperformed the regular ResNet-50, the drop in performance due to the high parameterisation and resulting high noise levels coupled with a much slower training does not justify its use (Table 3).

	ImageNette
ScaleNorm	44.2
No ScaleNorm	43.0

Table 3. Results of ResNet-50 and ScaleResNet-50 on ImageNette. $\epsilon=7.42$, 50 epochs, median of three runs.

E. Best-of-three

For completeness, we include the results of the best-performing ScaleResNet-9s, which typically showed larger separation from their regular counterparts compared to the median shown in the main manuscript, as seen exemplarily in Table 4.

	CIFAR-10 (ϵ 7.42)	ImageNette (ϵ 7.42)	Tiny ImageNet (ϵ 10)
ScaleNorm	72.4	66.1	42.8
No ScaleNorm	71.5	64.4	41.2

Table 4. Best of three runs classification performance on CIFAR-10, ImageNette and Tiny ImageNet (top-5).